64-Meter-Diameter Antenna With New Braces: Installation Description and Computed Performance for Gravity Loads

V. B. Lobb and M. S. Katow
DSIF Engineering Section

The performance of the 64-m antenna was improved for gravity loading by addition of two reaction bars or braces in the elevation wheel assembly. The installation is described. The performance is delineated in RF gain loss curves vs elevation angle changes from the 45-deg setting position of the Cassegrainian RF system. The gain loss curves were analytically calculated using distortion data computed by the NASTRAN program, which was then best-fitted by the RMS program.

I. Introduction

Based on predictions (Ref. 1) of improved performance of the 64-m antenna for gravity loadings, new reaction bars or braces were added in the elevation wheel assembly. The joints were designed to allow the major portion of the installation to be made during the nontracking time each day, with the final assembly being made at a shutdown period. The uncommonly large sizes and weights of the parts created special problems which required unique solutions.

In Ref. 1, only the direct solutions from the NASTRAN structural computing program consisting of the symmetric and the antisymmetric gravity loadings were given. In other words, the *OH* and *OZ* gravity components of Fig. 1 of 1.0 values were used and their respective distortion rms values were computed. (For definitions of symbols used in Fig. 1, see Tables 1 and 2). For comparisons of the performance to the field RF calibrations, the distortion rms must be computed as changes from the 45-deg elevation angle, which is the setting position of the surface panels of the paraboloid and the Cassegrainian RF system. Then, using the Ruze equation and the Radiation program, the performance degradation in dB may be computed.

II. Installation

The structural changes to the antenna were made by removing four existing knee bars and replacing them with two new braces (Fig. 49 of Ref. 1). For practical considerations, the design was modified, with the addition of another work point and cross bar to contain the resulting force component. The new braces (Fig. 2) and end joints (Fig. 3) are heavy structural members which weigh 1000 kg/m. These heavy weights and the need to field-drill 140 3.3-cm holes through material up to 7.6 cm thick required that work platforms be built and attached to the antenna. Because a large portion of the work was to be done without tracking interference, these work platforms were made of steel and left in place for 5 months. The site crane was used to erect the brace joints, which weighed from 2 to 4 metric tons each. During the shutdown of DSS 14 for hydrostatic bearing regrout, a 90-ton, 200-ft truck crane was used to erect the main braces which weigh 16 metric tons each. The brace connects to the elevation bearing casting. This presented a problem in getting an acceptable bearing area on a rough casting. Welding was considered and deemed feasible but was rejected because potential weld and casting cracking was deemed too risky. A special fixture (Fig. 4) was designed which adapted a milling head to special ways, which were attached to the casting and allowed a bearing surface to be machined into the casting.

Difficulty in finding a large impact wrench was encountered in installing the 300 3.2-cm high strength bolts, which require 7500 newtons of torque. A cross check of final installed bolted force was made by measuring the nut rotation. Many of the bolts were tightened using a slugging wrench and the turn-of-the-nut method.

III. Analysis

The distortion rms error was computed (Ref. 2) for the 75-deg elevation angle, for example, as shown in Fig. 1, by using for the equivalent gravity loading, the sum of the symmetric gravity vector $0Z$–$0Z'$ plus the antisymmetric vector $0H$–$0H'$. The best fit paraboloid moves off center to a position, also illustrated in Fig. 1 ,where a phase center offset occurs. This results in additional gain loss over that of the distortion rms of the surface panel support points about the best fit paraboloid.

Although an axial displacement of the phase center also occurs, little or no gain loss results because of a focusing operation by a Z-axial movement of the subreflector. This is done presently at the 64-m site only for operation at X and higher frequencies where there is a marked loss in gain by the axial defocused condition.

The Ruze gain loss equation used is

$$\text{Gain loss} = e^{-16\pi^2(\sigma/\lambda)^2}$$

where

σ = rms ½-pathlength error

λ = RF wavelength

For the phase center lateral offset, the Radiation program was used to compute the curve shown in Fig. 5.

Table 2 delineates the computations from the best fit paraboloid position, using for the basic phase center offset the calculated number for the 90-deg elevation case as described in Ref. 3.

IV. Analysis Results

To clearly define the effect of the structural modifications, the gain losses in equivalent rms distortion and dB of only the surface panel supporting points of the reflector structure were computed and delineated in Table 2 and by curves in Fig. 6. Figure 6 also shows the calculated curve for the premodification case.

For an additional step in improving the performance, the gain loss curve for zero lateral offsets is also shown. These theoretical values have not, as yet, been completely confirmed by field calibration. However, these corrections are practically feasible for the 64-m antenna since the tricone subreflector's lateral drives can be servoed with minor alterations. It should be noted that the resulting RF boresight direction changes must be compensated in the basic pointing system at the same time.

References

1. Katow, M. S., "210-ft-diam Antenna Reflector Upgrade Study—Phase 1," in *The Deep Space Network*, Space Programs Summary 37-62, Vol. II, pp. 109–113, Jet Propulsion Laboratory, Pasadena, Calif., Mar. 31, 1970.
2. Katow, M. S., and Schmele, L. W., "Antenna Structures: Evaluation Techniques of Reflector Distortions," in *Supporting Research and Advanced Development*, Space Programs Summary 37-40, Vol. IV, pp. 176–184, Jet Propulsion Laboratory, Pasadena, Calif., Aug. 31, 1966.
3. Katow, M. S., "64-m-Diameter Antenna: Computation of RF Boresight Direction," in *The Deep Space Network Progress Report*, Technical Report 32-1526, Vol. XIV, pp. 68–72, Jet Propulsion Laboratory, Pasadena, Calif., Apr. 15, 1973.

Table 1. Definition of symbols

D	rms distortion of surface panel support points
F	focus point of the best fit paraboloid
L	equivalent rms due to lateral offset of the phase center
MM	focal point offset from vertex
NN	RF phase center offset to focus of the best fit paraboloid
OG	full gravity vector
$O'G'$	full gravity vector
OH	antisymmetric gravity component at 45-deg elevation angle
$O'H'$	antisymmetric gravity component at 75-deg elevation angle
OZ	symmetric gravity component at 45-deg elevation angle
$O'Z'$	symmetric gravity component at 75-deg elevation angle
PP	RF phase center offset due to the Cassegrain system gravity deflections
V	vertex of the best fit paraboloid
VV'	vertex offset
WW	focal point offset from Z-axis of the basic coordinate system

Table 2. Best fit paraboloid data

Elevation angle, deg	X-rotation θ, rad	Y-offset VV', cm	MM, cm	WW, cm	PP, cm	NN, cm	Focal length, M	RMS		Gain	Loss	Total gain loss, dB
								D, mm	L, mm	D, dB	L, dB	
90	−0.002815	−12.909	7.63	−5.28	2.65	7.92	27.11625	0.50	1.21	−0.14	−0.79	−0.93
75	−0.001782	−8.166	4.83	−3.34	1.68	5.02	27.11562	0.35	0.77	−0.07	−0.33	−0.40
60	−0.000821	−3.762	2.22	−1.54	0.78	2.32	27.11324	0.18	0.35	−0.018	−0.067	−0.09
30	0.000627	2.864	−1.70	1.16	−0.60	−1.76	27.10398	0.20	0.27	−0.022	−0.040	−0.06
15	0.001016	4.636	−2.75	1.88	−0.97	−2.85	27.09773	0.40	0.44	−0.087	−0.105	−0.19
0	0.001142	5.195	−3.09	2.10	−1.10	−3.20	27.09095	0.60	0.49	−0.20	−0.13	−0.33

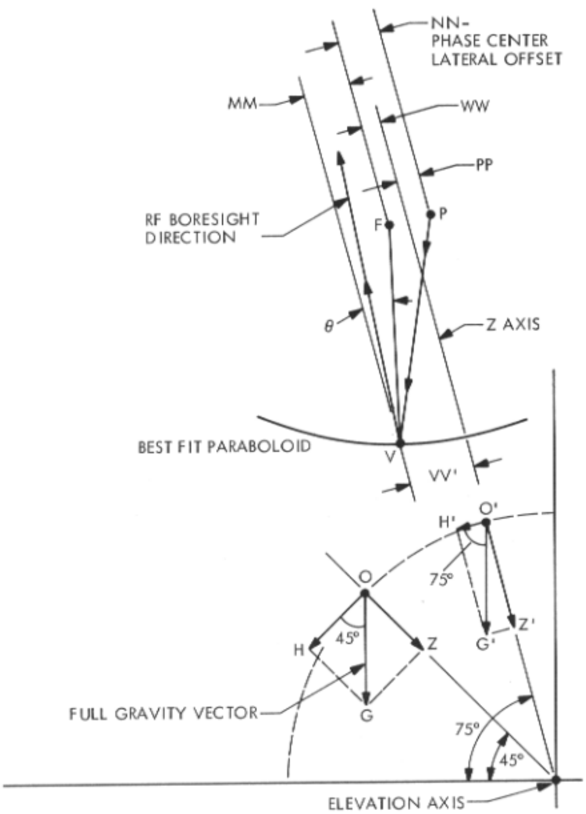

Fig. 1. The best fit paraboloid position and the gravity components

Fig. 2. New braces: 64-m-diam antenna

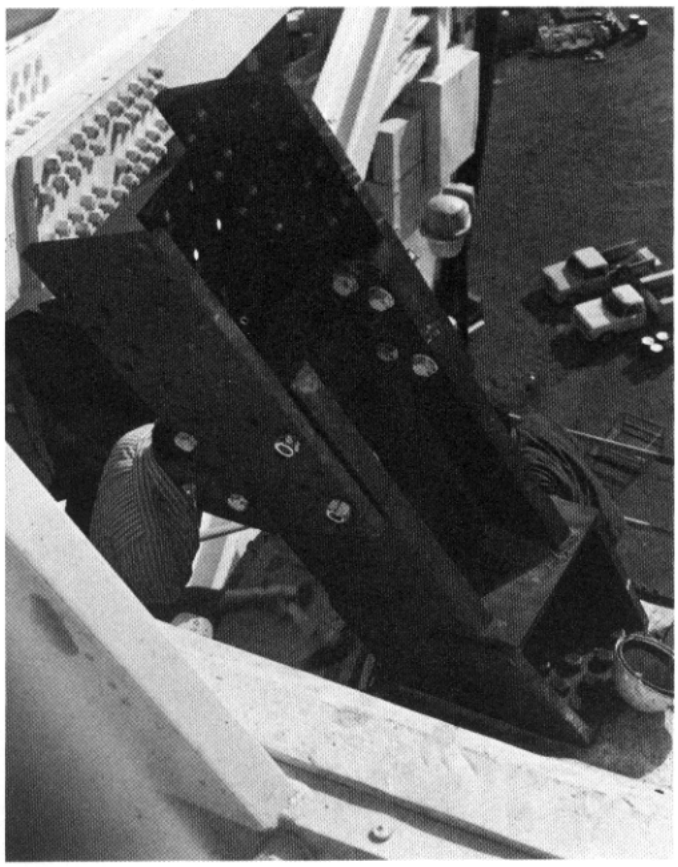

Fig. 3. New end joints: 64-m-diam antenna

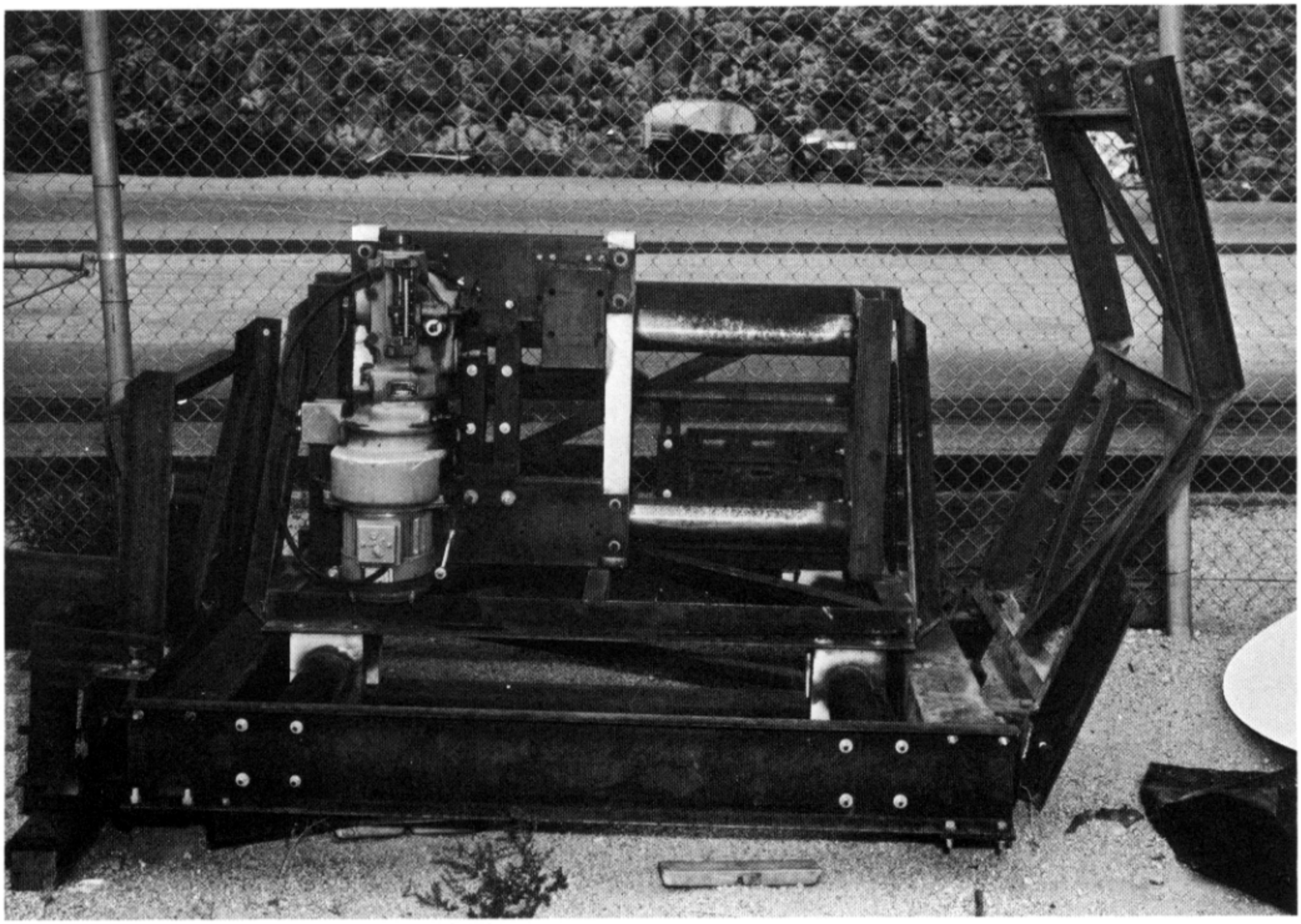

Fig. 4. Special fixture for milling elevation casting

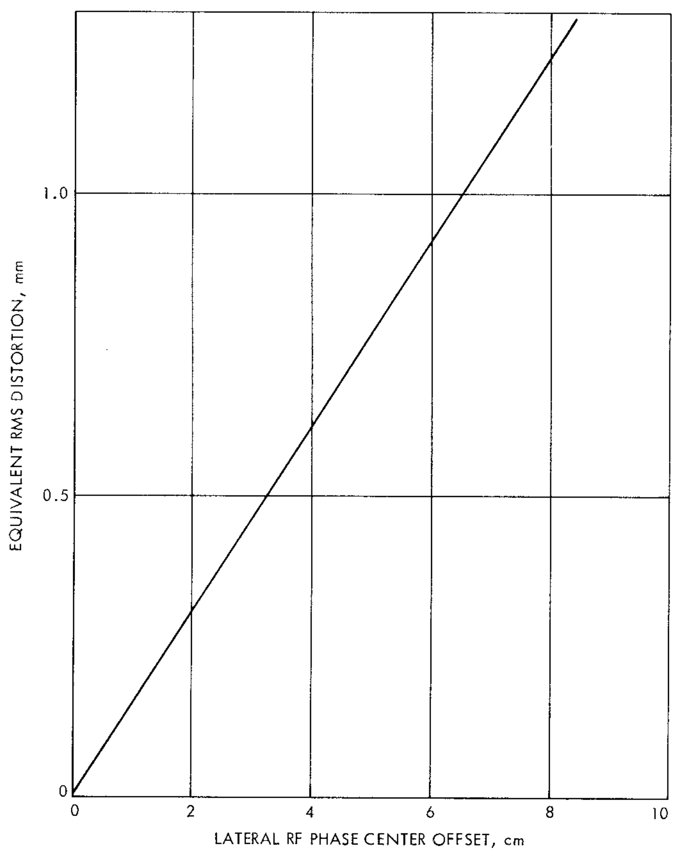

Fig. 5. RMS (equivalent) vs RF phase center offset

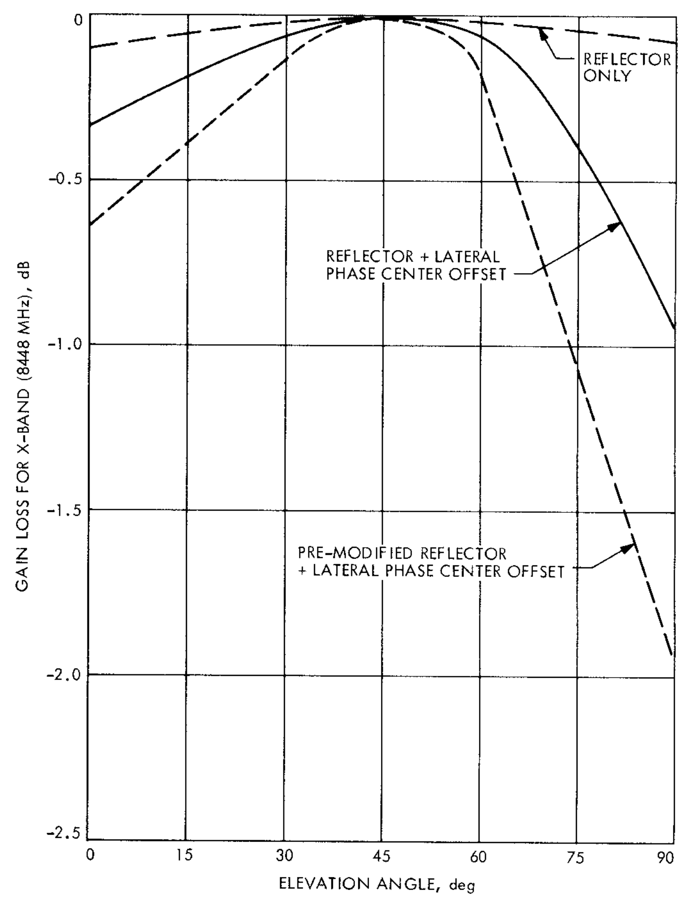

Fig. 6. Gain loss vs elevation angle